

Langmuir Layers and Langmuir–Blodgett Films of Bis-tetrathiafulvalene Annelated Macrocycle

Takayoshi Nakamura,*[,1,2,3] Yoko Tatewaki,[2] Takanori Ohta,[2] Keisuke Wakahara,[4] Tomoyuki Akutagawa,*[,1,2] Tatsuo Hasegawa,[1,2] Hiroaki Tachibana,[5] Reiko Azumi,[5] Mutsuyoshi Matsumoto,[3,5] Christian A. Christensen,[6] and Jan Becher[6]

[1]Research Institute for Electronic Science, Hokkaido University, Sapporo 060-0812

[2]Graduate School of Environmental Earth Science, Hokkaido University, Sapporo 060-0810

[3]CREST, Japan Science and Technology Corporation (JST), Kawaguchi 332-0012

[4]Graduate School of Science, Hokkaido University, Sapporo 060-0810

[5]National Institute of Advanced Industrial Science and Technology (AIST), Tsukuba Central 5, Tsukuba, Ibaraki 305-8565

[6]University of Southern Denmark, Campusvej 55, DK-5230, Odense M, Denmark

Received July 29, 2004; E-mail: tnaka@imd.es.hokudai.ac.jp

The Langmuir layers of amphiphilic bis(tetrathiafulvalene) [bis(TTF)] annelated macrocycle (**1**) and those of the (**1**)[2,3,5,6-tetrafluoro-7,7,8,8-tetracyano-*p*-quinodimethane (F_4-TCNQ)]$_2$ charge-transfer (CT) complex were evaluated. The neutral molecule of **1** recognized Cs^+ ion at the air–water interface forming a domain structure. Contrastingly, (**1**)(F_4-TCNQ)$_2$ did not recognize Cs^+ ion at the air–water interface. The Langmuir layers of **1** were deposited on a mica surface, resulting in the formation of fibrils. The highly oriented structure of the fibrils at the molecular level was confirmed by a large dicroism in the IR spectra. The (**1**)(F_4-TCNQ)$_2$ layer deposited on the mica surface consisted of nanowires oriented in specific directions. The UV–vis–NIR spectra revealed an intramolecular dimer structure of the donor **1** cation radical in the CT complex. An extended nanowire network structure was obtained when the K^+ cation was introduced into the subphase. The stacking of intramolecular TTF dimers and intermolecular F_4-TCNQ dimers directed the formation of nanowires, which are oriented on mica by recognizing fully occupied hexagonal K^+ sites at the surface. The nanowire orientation was readily disturbed by varying film deposition conditions such as subphase temperature, deposition speed, or surface pressure, indicating that the fluidity of Langmuir layer was important for obtaining nanowire structure.

Nanowire, one of the key materials for future nanoelectronic devices,[1] has been extensively studied recently.[2] A wide range of materials, from metals to semiconductors and carbon nanotubes, are utilized in nanowire formation.[2,3] Systems using crossbar configurations have been previously reported in connection with their applications to semiconductor nanowires.[4–6] When a p–n junction was fabricatied in a crossbar-configuration using p- and n-doped GaAs nanowires, a rectification was observed.[5] The junction was also used as an FET showing an ON/OFF ratio of 10^5 at a 1 V gate voltage.[6] Carbon nanotubes exhibit metallic or semiconducting properties based on the chirality of C–C bonds, and rectifiers are fabricated from a single carbon nanotube.[7] Nonvolatile random access memories were constructed from carbon nanotube crossbar-configurations.[8] Organic materials are also good candidates for nanowire formation. Conducting polymers such as poly(pyrrole) and poly(thiophene) tend to form fibrous structures, which are utilized for nanowire formation.[9] For example, poly(pyrrole) wires having a 50-nm diameter have been successfully synthesized by regulating electrochemical polymerization potentials.[9b] One of the advantages of utilizing organic materials is that we can design and synthesize molecules with appropriate functions. In this context, molecular conductors are promising materials for application of nanowire construction in the future. Electron donor or acceptor charge-transfer (CT) complexes yield highly conducting single crystals with metallic properties.[10] In the crystals, molecules often form one-dimensional (1D) π-stacking columns, which give a quasi-1D π-band structure due to π-orbital interaction along the stacking axis. The crystals have needle-like structures, consistent with the 1D stack of the π-molecules, which are suitable for fabricating nanowires. Indeed, highly conducting tetrathiafulvalene (TTF) bromide salt nanocrystals with diameters down to 25 nm have been prepared by the electrocrystallization method using a platinum nanoparticle electrode.[11]

We recently reported a novel nanowire structure utilizing the CT complex of amphiphilic bis(tetrathiafulvalene) [bis(TTF)] annelated macrocycle (**1**) (Scheme 1) and 2,3,5,6-tetrafluoro-7,7,8,8-tetracyano-*p*-quinodimethane (F_4-TCNQ), (**1**)(F_4-TCNQ)$_2$, by using the Langmuir–Blodgett (LB) method.[12–14] Upon transfer of the Langmuir layers from the 0.01 M KCl aqueous subphase to mica substrates, nanowire structures with

Published on the web February 11, 2005; DOI 10.1246/bcsj.78.247

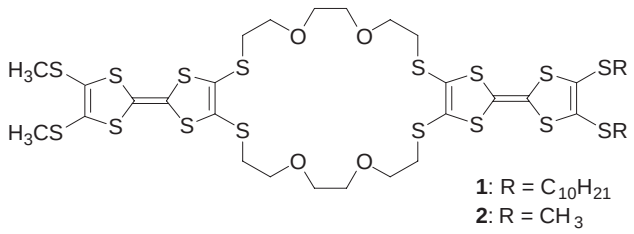

Scheme 1. Bis(TTF) annelated macrocyles (**1**) and (**2**).

the typical dimensions of $2.5 \times 50 \times \sim 1000$ nm^3 were developed. These nanowires recognize mica surface and are oriented in specific directions, forming 60° angles to one another.

Molecule **1** was designed to possess both electronic-conduction and ion-recognition ability. The TTF moiety of **1** is expected to exhibit high electrical conductivity in its partially charged state by forming a 1D columnar structure in the solid state. Macrocyclic polyether molecules have an ability to recognize metal ions in solution according to the relationship between the size of the macrocyclic cavity and the radius of the ion.[15] For example, [18]crown-6 and [15]crown-5 recognize potassium and sodium cations in solution, respectively. Like dibenzo-[24]crown-8, the 24-membered ring in molecule **1** is thought to be suitable for recognizing a Cs^+ cation.[16] However, the relationships between these properties and the mechanism of nanowire formation have not been explained yet.

Herein, we describe the detailed surface properties of the Langmuir layers and Langmuir–Blodgett films of the (**1**)(F_4-TCNQ)$_2$ CT complex and of neutral molecule **1**. The ion-recognition abilities of Langmuir layers to Cs^+ cations of both the neutral **1** and CT complex were examined from the surface pressure-area (π–A) isotherm and by Brewster angle microscope (BAM). The morphologies of transferred films on mica surfaces were investigated by atomic force microscope (AFM) and the ordered structures at the molecular level of these films were revealed by spectroscopic measurements. Preparation conditions of nanowires in terms of fluidity of Langmuir layers are discussed.

Experimental

General. A conventional LB trough (NIMA 5152D) was used for π–A isotherm measurements and LB film depositions. Spectroscopic grade $CHCl_3$–CH_3CN (9:1) mixture was used as a spreading solvent; the concentration of spreading solutions was adjusted to 0.5 mM with respect to **1**. The (**1**)(F_4-TCNQ)$_2$ complex was prepared in-situ by combining **1** and two equivalents of F_4-TCNQ in a spreading solution. The π–A isotherms were recorded at a compression speed of 20 mm min^{-1} at 290 K. Langmuir layers were transferred on freshly cleaved mica substrates by the vertical dipping method with a deposition speed of 10 mm min^{-1}, these substrates were subjected to AFM measurements. The horizontal lifting method was used for the preparation of the LB films for spectral measurements. Film transfer was carried out at 290 K unless otherwise noted.

Atomic Force Microscopy and Brewster Angle Microscopy. AFM images were taken by a Seiko SPA 400 with an SPI 3800 probe station in tapping mode (dynamic force mode). Commercially available Si cantilevers with a 13 N m^{-1} force constant were used. Surface morphologies of the films transferred onto mica by a single withdrawal were observed as topographic images. BAM images were taken by an instrument constructed in-house. The images are 1.5×1.0 mm^2.

Optical Spectra. Polarized UV–vis–NIR (300–3000 nm) and IR (400–7800 cm^{-1}) spectra were measured with a Perkin-Elmer Lamda-19 and a Perkin-Elmer Spectrum 2000 spectrometers, respectively. The 20-layer LB films were transferred onto quartz (20×13 mm^2) for UV–vis–NIR measurements. Polarized UV–vis–NIR spectra were measured using *p*- and *s*-polarized light at an angle of incidence of 45° (45*p* and 45*s*). For IR measurements, transmission (*T*) and reflection–absorption (*RA*) spectra of 20-layer LB films were measured on CaF_2 and evaporated Au substrates, respectively. Spectra were recorded by 2000 scans of an MCT detector with a 4 cm^{-1} resolution. An angle of incidence of 80° was used for *RA* measurements.

Results and Discussion

Langmuir Layers on Aqueous Subphase. As reported previously,[12] molecule **1** shows a reversible two-step two-electron redox reaction. We consider four states (**I**–**IV**) of molecule **1** determined by the oxidation state of TTF moieties and ion-recognition states of the macrocyclic region (Scheme 2). In the present study, we achieved the cation radical state of **1** by adding two equivalents of a relatively strong electron acceptor, F_4-TCNQ, to the spreading solution forcing a complete electron transfer from the TTF moiety to F_4-TCNQ.[12] The macrocyclic moiety may recognize ions present in the subphase during Langmuir layer formation and deposition. We selected Cs^+ ion for the ion-recognition study, because the [24]crown-8 ring system of molecule **1** usually has higher ion-recognition ability for Cs^+ than other alkali metal ions.[15]

The π–A isotherms for states **I**–**IV** resulted in Langmuir layer formation at the air–water interface in all cases (Fig. 1). We used a subphase of 0.01 M CsCl solution at states **II** and **IV**. A neutral molecule on a pure water surface (state **I**) gave a limiting area of 0 mN m^{-1} as $A_0 = 0.60$ nm^2. Contrastingly, when 0.01 M CsCl was used as the subphase (state **II**), the lift-off point of the π–A isotherm was larger than that on pure water, suggesting ion-recognition of molecule **1** at the air–water interface.

To evaluate the Cs^+ ion-recognition ability of Langmuir layer **1**, we examined the Cs^+ concentration dependence of the π–A isotherms. Figure 2 shows the π–A isotherms of molecule **1** at various CsCl subphase concentrations. The π–A isotherms of molecule **1** with CsCl in the subphase are almost identical to that of molecule **1** on pure water up until a Cs^+ concentration of 2×10^{-4} M. An abrupt jump in the lift-off point was observed at a CsCl concentration around 4×10^{-4} M.

Figure 3 shows the BAM images of Langmuir layer of **1** at 5 mN m^{-1} on a subphase supplemented with CsCl at various concentrations. Formation of domain structures was observed in the Langmuir layers on a 1×10^{-3} M CsCl aqueous subphase. Domain formation is thought to be associated with the ion-recognition of molecule **1** at the air–water interface. When the Cs^+ ion concentration was increased to 1×10^{-2} M, the π–A isotherm changed significantly. A similar π–A profile was also observed in the Langmuir layer at CsCl concentrations of 1×10^{-1}. The change in π–A profile was reflected in the BAM images (Figs. 3(d), (e)).

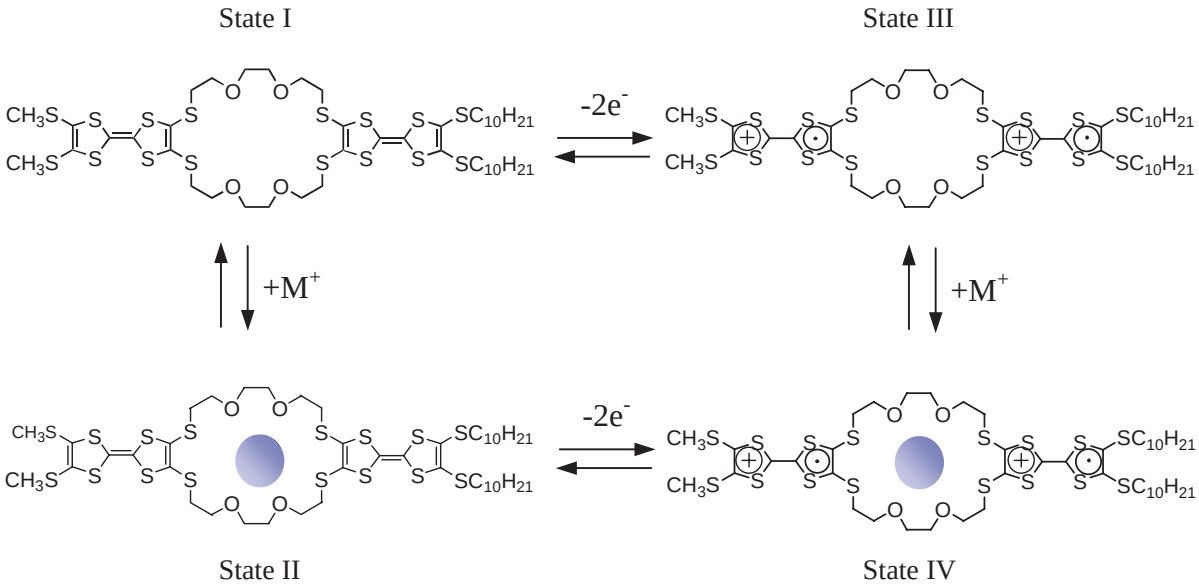

Scheme 2. Four redox and ion-recognition states of compound **1**. Vertical and horizontal reaction pathways correspond to ion-recognition and charge-transfer interactions, respectively.

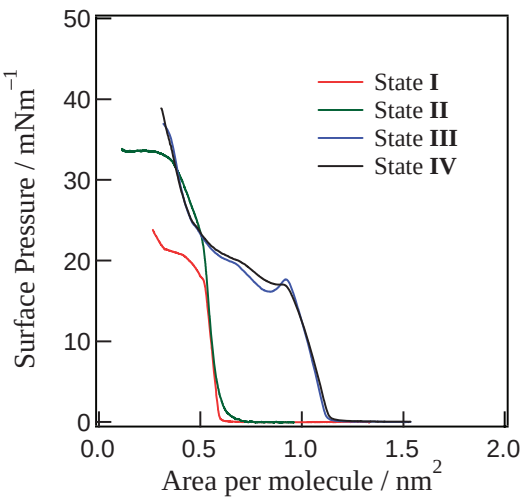

Fig. 1. π–A isotherms of states **I**–**IV**.

The π–A isotherm started to rise at larger area (1.15 nm^2) upon CT complex formation (state **III**), indicating that the two additional F_4-TCNQ molecules affected the molecular area. In state **IV**, the π–A isotherms did not change significantly upon increasing the concentration of CsCl in the subphase up to 1 M, suggesting that Cs^+ ion-recognition ability of (**1**)(F_4-TCNQ)$_2$ is rather poor compared to that of neutral molecule **1**. Therefore, state **IV** in its ideal form does not seem to be achieved at the air–water interface, although we refer to the film as state **IV** throughout the manuscript. This assumption has been further confirmed by observing the BAM image, as the morphology of the Langmuir layer did not change significantly compared to that without Cs^+ ions.

Film Morphology on Mica Surface. Next, we transferred Langmuir layers in the four states to mica substrates and examined the surface morphology of each film by AFM at the mesoscopic level. Figure 4 shows the AFM images of films transferred at 10 mN m^{-1}. Significant differences in the surface mor-

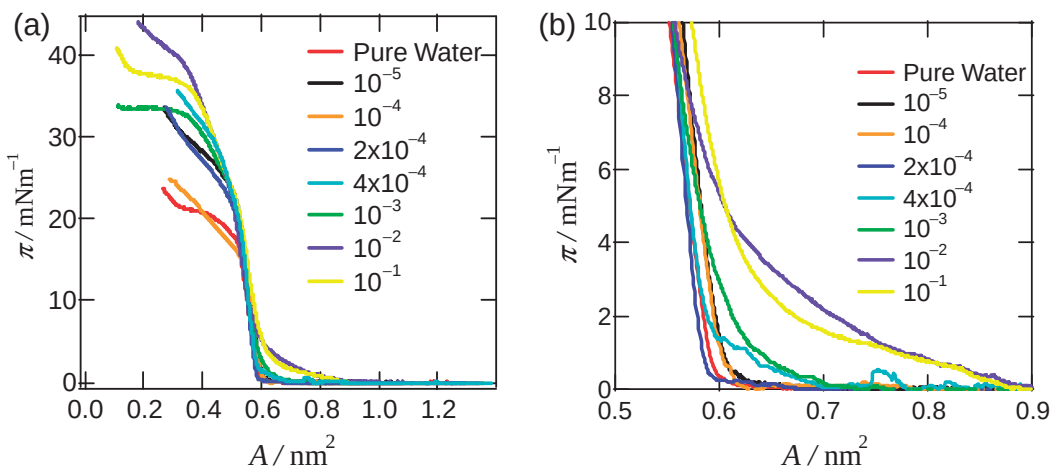

Fig. 2. The π–A isotherms of molecule **1** on pure water and of molecule **1** with CsCl in the subphase (a). The expansion of low surface pressure region (b).

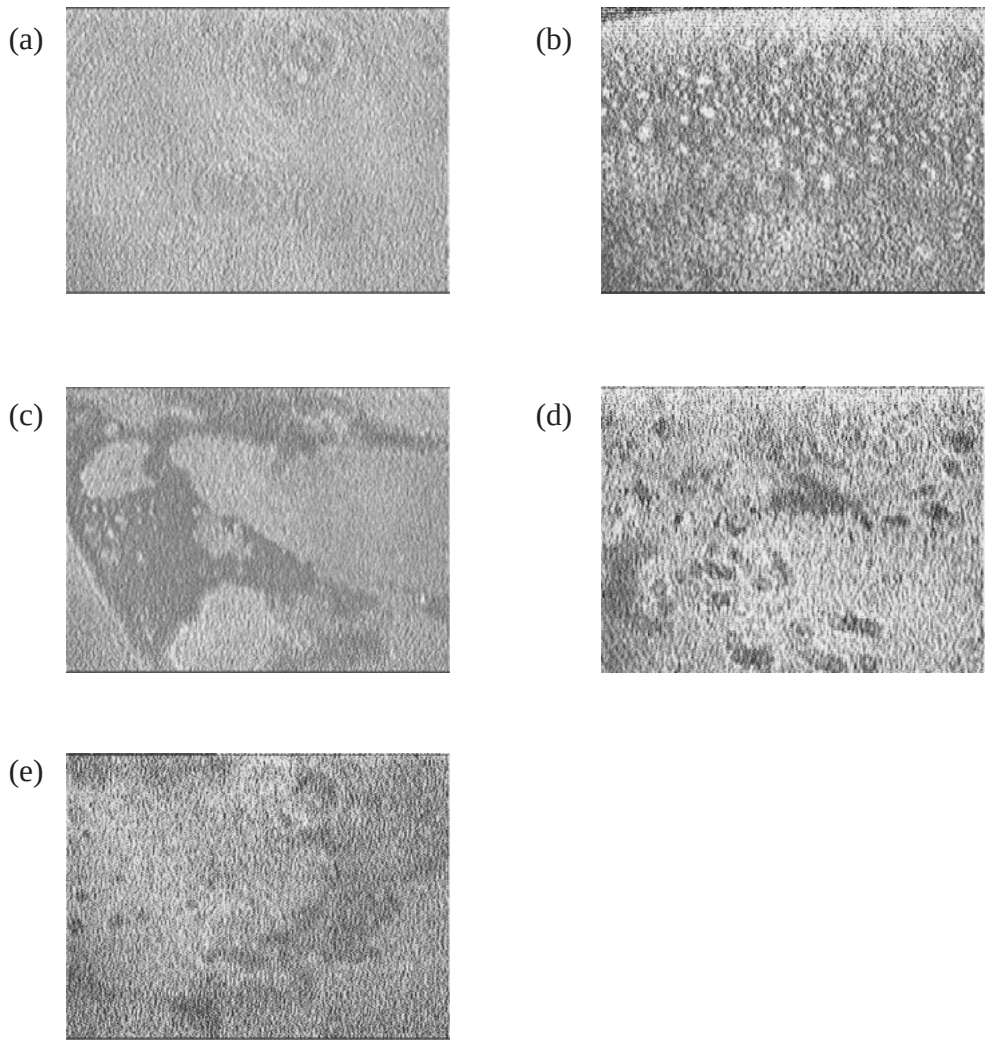

Fig. 3. BAM images of Langmuir layers ($\pi = 5$ mN m^{-1}) of **1** a) on pure water and on CsCl supplemented aqueous solution b) at 1×10^{-4}, c) at 1×10^{-3}, d) at 1×10^{-2}, and e) at 1×10^{-1} M. The images are 1.5×1.0 mm^2.

phology were observed between neutral molecule **1** and (**1**)(F_4-TCNQ)$_2$. In state **I**, the film is composed of small fibrils, forming micrometer size domains on the substrate. Upon addition of CsCl to the subphase (state **II**), small fibrils covered the entire substrate. However, in both cases, each fiber had almost an identical shape, with the height of 2 nm and typical width of 50 nm.

Upon examination of the CT complex (state **III**), elongated fibrils with a typical width of 50 nm are evident. The bundles of fibers form circles with some fibers extended. The typical height of the fibers is around 3 nm. Upon introduction of Cs^+ cations in the subphase, the fibers are elongated and oriented on the mica surface. Since fibers are expected to have semiconducting propertes, we can regard the resultant structures as oriented nanowires. The majority of nanowires are aligned on the mica surface so as to form angles of 60° to each other. As previously mentioned, the CT complex may not recognize Cs^+ ions at the air–water interface. Furthermore, since the orientation of the wires was consistent with the crystal axes of mica,[17] the nanowires orient themselves during the film deposition processes.

UV–Vis–NIR and IR Spectra of LB Films. To evaluate the structure at the molecular level and the electronic structure of the film deposited from states **I**–**IV**, we measured the electronic and vibrational spectra. Polarized electronic spectra of the LB films measured in the UV–vis–NIR region are shown in Fig. 5. Since the spectra of states **I** and **III** were identical to those of states **II** and **IV**, only the spectra of states **I** and **IV** are shown. It is reasonable that states **III** and **IV** have the same spectra considering the poor Cs^+ ion-recognition ability of the (**1**)(F_4-TCNQ)$_2$ CT complex. However, in state **II**, spectral changes relative to state **I** are expected due to the ion-recognition ability of molecule **1**. We measured the Cs^+ ion content in the LB film surface of state **II** by XPS (X-ray photoelectron spectroscopy) and found that film contained almost no Cs^+ ions. This indicates that the Cs^+ ions are dissociated from molecule **1** during the film deposition process. That the shapes of the fibrils as seen in the AFM images of states **I** and **II** are similar further supports this conclusion.

The UV–vis–NIR spectra of state **I** exhibited two bands at 23.3 and 32×10^3 cm^{-1}, representing the intramolecular transitions of TTF macrocycles, because absorptions around 25 and 33×10^3 cm^{-1} have been reported in neutral TTF in

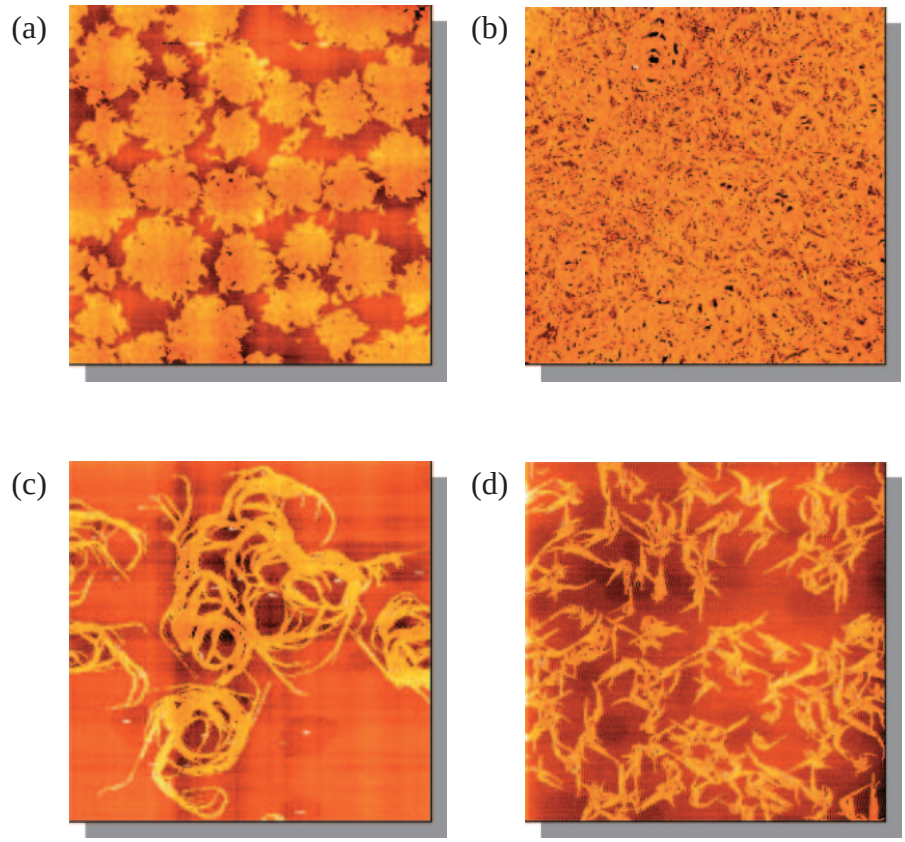

Fig. 4. AFM images of the films transferred onto a mica surface by single withdrawal from the monolayers at the air–water interface in a) state **I**, b) state **II**, c) state **III**, and d) state **IV**. The images are 10×10 μm^2.

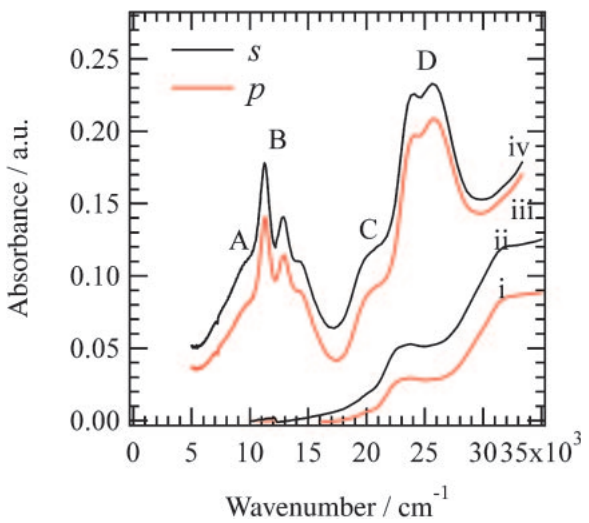

Fig. 5. Polarized transmission UV–vis–NIR spectra of 20-layer LB films at 45° angles of incidence. The spectra of the film of state **I** with i) *p*- and ii) *s*-polarized light and those of state **IV** with iii) *p*- and iv) *s*-polarized light.

CH_3CN solution.[18] No in-plane anisotropy was observed at normal incidence, showing the isotropic molecular-orientation distribution on the substrate surface. With the *p*- and *s*-polarized light at an angle of incidence of 45°, the intensity of each absorption band with *s*-polarized light was larger than that with *p*-polarized light. Since the intramolecular transition moment of the TTF is along the long axis of the molecule,[18] the long axes of TTF moieties are considered to be parallel to the substrate surface.

A completely ionic ground state of $(\mathbf{1}^{2+})(F_4\text{-}TCNQ^-)_2$ was expected for state **III** and **IV** film based on the difference of redox potential between the first-wave oxidation potential of molecule **1** (0.56 vs SCE in $C_2H_4Cl_2$) and the first-wave reduction potential of F_4-TCNQ (0.73 V vs SCE in $C_2H_4Cl_2$).[19] In fact, the **A**-band appeared at 9×10^3 cm^{-1} as a shoulder, which was also observed in the completely ionic crystalline $(\mathbf{2}^{2+})(I_3^-)(I_5^-)$ CT complex reported previously.[20] The $(\mathbf{2}^{2+})(I_3^-)(I_5^-)$ CT complex formed an intramolecular dimer in the crystal, whose **A**-band appeared at 9×10^3 cm^{-1}.[20] Therefore, the **A**-band of the LB film is assigned to the intramolecular transition of the intramolecular dimer in the TTF^+ moieties.

Two sharp absorptions (**B**-bands) at 11.2 and 12.9×10^3 cm^{-1} are assigned to the intramolecular transition of the F_4-TCNQ anion radical, in which the absorption bands were observed at 11.4 and 13.1×10^3 cm^{-1} in CH_3CN solution.[21] The **C**- and **D**-bands that appear at 21 and 23.5 (26.0) $\times 10^3$ cm^{-1}, respectively, are assigned to the intramolecular transitions of TTF^+ and F_4-$TCNQ^-$. No in-plane anisotropy of state **IV** was observed at normal incidence, indicating that the complex is oriented isotropically on the substrate surface. At an angle of incidence of 45°, the intensity of each absorption band is larger for the *s*-polarization than that for the *p*-polarization.

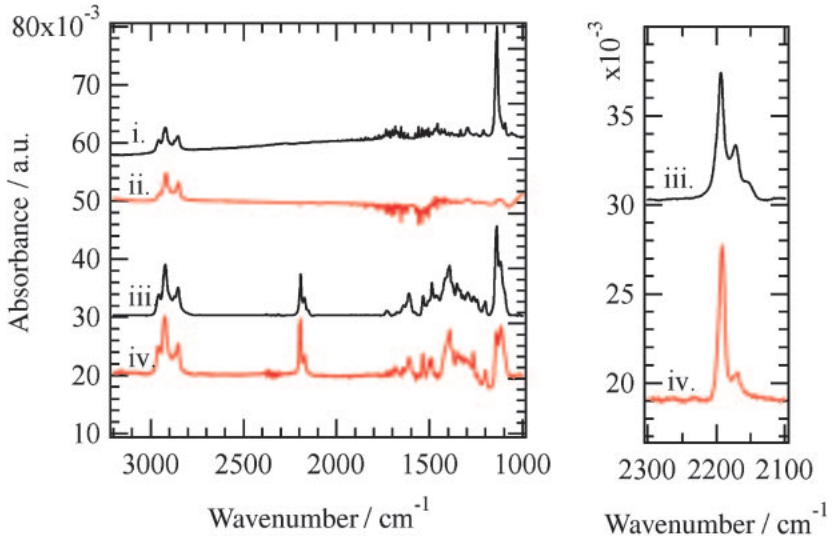

Fig. 6. Transmission (*T*) and reflection-absorption (*RA*) spectra in the energy range from 3200 to 1000 cm^{-1} (left) and from 2300 to 2100 cm^{-1} (right) of the film. i) *RA*- and ii) *T*-spectra of state **I**, iii) *RA*- and iv) *T*-spectra of state **IV**. Baselines are corrected.

Since the observed intramolecular transition moments of the donor and F_4-TCNQ are along the long axes of TTF units and F_4-TCNQ molecules, the long axes of TTF moieties of molecule **1** and F_4-TCNQ are parallel to the substrate surface. The LB film in state **III** showed dichroic spectra identical to that of the LB film in state **IV**, indicating the same molecular orientation within the LB films.

The molecular orientation of the molecule in the LB film was evaluated by transmission (*T*) and reflection-absorption (*RA*) IR spectra.[22] Figure 6 shows the transmission (*T*) and reflection-absorption (*RA*) IR spectra of LB film in states **I** and **IV**. The transition moments parallel to the substrate surface are activated in the *T*-spectra, while those normal to the substrate surface are enhanced in the *RA*-spectra. In both optical arrangements, symmetric and asymmetric ν_{CH_2} bands of *n*-$C_{10}H_{21}S$– chains and CH_2CH_2 moieties in the macrocyclic unit were observed at 2922 and 2852 cm^{-1}, respectively.[22,23] We may estimate the average orientation angle of the C–H bonds from these spectra. However, since the bands originated both from the methylene units of alkyl chains and from the macrocyclic units, the orientation of each methylene unit cannot be determined. The mode observed at 1140 cm^{-1} may be assigned to the C–O–C asymmetric stretch of the macrocyclic unit,[24] which showed a strong dicroism in state **I**. Although quantitative analysis is difficult due to the overlap with the other modes in the *T*-spectrum, the strong absorption of the band observed only in the *RA*-spectrum indicates an almost perpendicular orientation of C–O–C region of the macrocyclic unit with respect to the substrate surface, predominantly in state **I**. The strong dicroism also indicates a well-ordered structure of the fibrils at the molecular level in state **I**.

Two kinds of ν_{CN} bands of LB film were observed at 2172 and 2194 cm^{-1}; these can be assigned to b_{1u}- and a_g-modes, respectively, in state **IV**.[25] Since the ν_{CN} (a_g) band of neutral F_4-$TCNQ^0$ and ionized F_4-$TCNQ^-$ have been observed at 2227 and 2193 cm^{-1}, respectively,[25] the electronic ground state of F_4-TCNQ in state **IV** is close to the completely ionic state. Although the a_g-mode is usually forbidden in the IR spectra, the lattice distortions such as dimerization of F_4-TCNQ should activate the a_g-mode by breaking the symmetry of the molecular environment. We have reported the crystal structure of closely related $(\mathbf{2}^{2+})(F_4\text{-}TCNQ^-)_2$ CT complex, in which F_4-TCNQ forms a dimer. The activation of F_4-TCNQ a_g-modes as well as the **A**-band that appeared in the NIR region due to the TTF dimer indicates that molecule **1** and F_4-TCNQ in the nanowires have similar molecular orientations and configurations to the $(\mathbf{2}^{2+})(F_4\text{-}TCNQ^-)_2$ crystal.[12]

Mechanism of Nanowire Formation. In state **IV**, we observed an oriented nanowire structure when Cs^+ cations were introduced into the subphase. The morphology of nanowires on mica surfaces is strongly dependent on the cation species in the subphase.[12] The π–*A* isotherms on aqueous subphases containing 0.01 M LiCl, KCl, CsCl, and $BaCl_2$ did not show significant differences from one to another. However, when we introduced K^+ cations in the subphase, highly oriented nanowire network structures were observed.

Mica is typically composed of $KAl_3Si_3O_{10}(OH)_2$, and vacant K^+ sites of six-fold symmetry appear by cleavage.[17] These sites are negatively charged, thereby attracting cations when the mica substrates are immersed in cation-containing subphases. Upon introduction of Li^+ or Cs^+ cations in the subphase, the cation sites are not completely filled due to the difference between the cation size and the empty pocket; the radius of a Li^+ ion is 0.6 Å and that of a Cs^+ ion is 1.69 Å, whereas that of a K^+ ion is 1.33 Å. Although the ion radius of Ba^{2+} (1.35 Å) is almost the same a that of K^+, Ba^{2+} ions do not fill the cation sites due to the difference in cation charge. Therefore, the nanowire orientation on a mica surface completely disappeared in the LB for films transferred from a $BaCl_2$-supplemented subphase.[12] Although the $(\mathbf{1})(F_4\text{-}TCNQ)_2$ does not recognize ions at the air–water interface, the above results indicate that the nanowire recognizes fully occupied K^+ sites on the mica surface and gives an oriented structure. In accordance with both the molecular structure of **1** and the spectral analysis described above, π-stacking of the TTF intramolecular dimer with F_4-TCNQ intermolecular dimer is con-

sidered to be the origin of the nanowire formation, although the mechanism of formation of nanowire morphology with specific dimensions is not clear at present.

Since the nanowire network structure was observed by introducing K^+ ions in the subphase, we examined the conditions for film deposition to clarify the best conditions for the fabrication of a nanowire network structure. First, we examined temperature, ion concentration in the subphase and deposition speed for film transfer. The extended nanowire network formation was observed only in limited conditions. When we varied the subphase temperature, the morphology of the transferred film changed significantly, and the extended nanowires were obtained in a very narrow subphase temperature range, around 291 K. The concentration of K^+ ion in the subphase also affected nanowire formation. The concentration of 10^{-3} M was too low to obtain extended nanowires. A higher concentration, 0.1 M, also interrupted nanowire formation. Extended nanowires were formed when Langmuir layers were deposited at a withdrawal speed of 10 mm/min. Deposition speeds of 5 mm/min or 20 mm/min suppressed nanowire formation, suggesting that the sheer stress upon the film deposition plays an important role in the growth of extended nanowire network structures.

Figure 7 shows the AFM images of nanowires transferred at different pressures. At low pressures, thick nanowires form cyclic domains, whereas extended nanowires are evident when the Langmuir layers are deposited around 10 mN/m. The extended structures tend to be destroyed at higher pressures, and the entire substrate is covered with small fibrils when the film is deposited above 20 mN m^{-1}. Since high surface pressure as well as high ion concentration hinders the nanowire formation, fluidity of the Langmuir layers is a critical parameter for nanowire formation. The narrow temperature range of the subphase and the limited deposition speed for obtaining nanowires should also be related to the fluidity of the Langmuir layers. These results strongly suggest that we can control the morphology of the nanowire network by regulating the conditions of film deposition.

Conclusion

We described the surface properties of the Langmuir layers of the CT complex of amphiphilic bis(TTF) annelated macrocycle (**1**) and F_4-TCNQ in comparison with neutral molecule **1**. In neutral form, the Langmuir layer at the air–water interface recognizes Cs^+ ions in the subphase forming a domain structure. On the basis of the results of both π–A isotherms and BAM images, we concluded that the (**1**)(F_4-TCNQ)$_2$ Langmuir layers do not recognize Cs^+ ions. However, the layer deposited on the mica surface consisted of nanowires oriented in specific directions, that recognize the ion array on the surface. The morphology is dependent on the cationic species in the subphase, and an extended nanowire network structure is obtained upon introduction of potassium cations, which fill their sites on mica surface.

The spectral analysis of the deposited films reveals the structure at the molecular level. A highly oriented structure at the molecular level is confirmed by a large dichroism in IR spectra of neutral molecule **1**. In the charge transfer complex, the cation radical of molecule **1** forms an intramolecular dimer structure and F_4-TCNQ also forms a dimer. The stacking structure of these dimers are considered to give the formation of nanowires, which are oriented on the mica surface by recognizing fully occupied K^+ sites.

The orientation of the nanowires is readily disturbed by the changes in conditions of film deposition such as subphase temperature, deposition speed, and surface pressure. This suggests

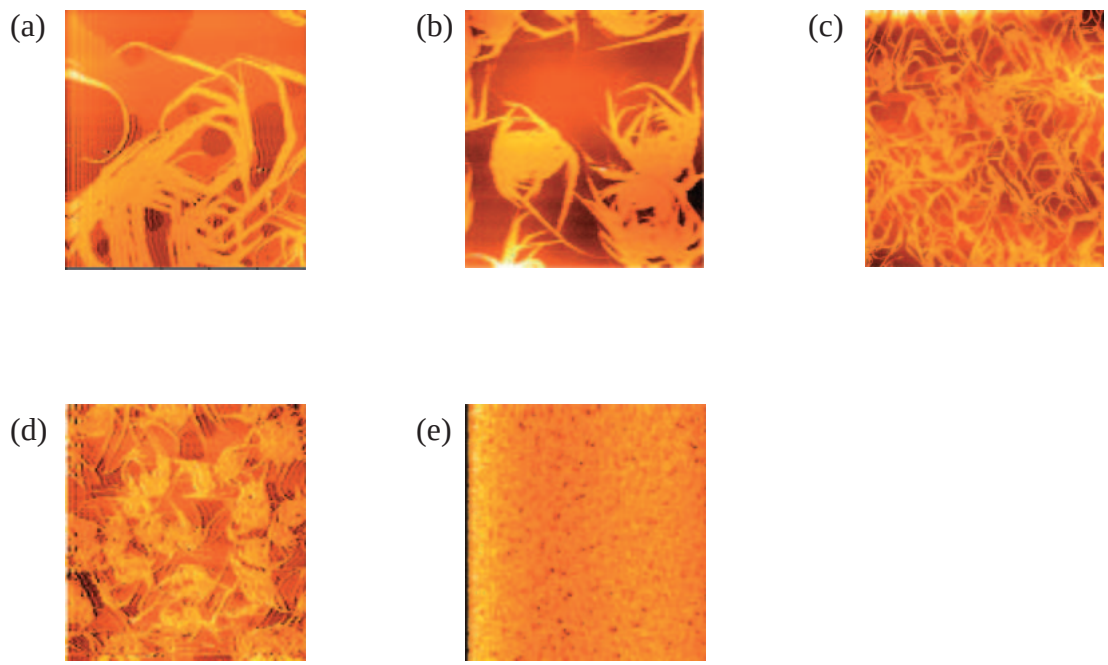

Fig. 7. Deposition pressure dependence of the surface morphology of the nanowires. A 0.01 M KCl subphase solution was used and the films were deposited at 291 K, at a deposition speed of 10 mm min^{-1}. Deposition pressure was a) 1, b) 5, c) 10, d) 15, and e) 20 mN m^{-1}. The scale for all AFM images is 10 × 10 μm^2.

that the fluidity of the Langmuir layers is a critical parameter for nanowire formation and that we can control the morphology of nanowire networks by controlling these conditions.

Although we have succeeded in fabricating a nanowire network structure, the wires are semiconducting due to the full charge transfer state of the (**1**)(F_4-TCNQ)$_2$ complex. The next step may be to obtain highly conducting nanowires by optimizing the partial charge transfer state of the complex through chemical modification of the donor and acceptor. Chemical modification studies are currently underway.

The authors are grateful to Dr. Hiroshi Yokoyama, National Institute of Advanced Industrial Science and Technology, for his help in constructing the BAM equipment used for this study. This research was supported in part by a Grant-in-Aid for Science Research from the Ministry of Education, Culture, Sports, Science and Technology and by the Proposal-Based New Industry Creative Type Technology R&D Promotion Program from the New Energy and Industrial Technology Development Organization (NEDO) in Japan. A grant from the Danish National Science Research Council (SNF) to J. B. is also gratefully acknowledged.

References

1 a) T. Akutagawa and T. Nakamura, "Semiconductor and Molecular Assembly Nanowires in Chemistry of Nano-molecular Systems—Toward the Realization of Molecular Devices," ed by K. Sugiura, T. Matsumoto, H. Tada, and T. Nakamura, Springer-Verlag, Berlin (2002), p. 123. b) C. Joachim, J. K. Gimzewski, and A. Aviram, *Nature*, **408**, 541 (2000).

2 Recent progress in nanowires. See special issue of nanowires in *Adv. Mater.*, **15**, issue 5 (2003).

3 J. Hu, T. W. Odom, and C. M. Lieber, *Acc. Chem. Res.*, **32**, 435 (1999).

4 a) J. R. Heath, P. J. Kuekes, G. S. Snider, and R. S. Williams, *Science*, **280**, 1716 (1998). b) N. A. Melosh, A. Boukai, F. Diana, B. Gerardot, A. Badolato, P. M. Petroff, and J. R. Heath, *Science*, **300**, 112 (2003).

5 Y. Cui and C. M. Lieber, *Science*, **291**, 851 (2001).

6 Y. Huang, X. Duan, Y. Chi, L. J. Lauhon, K. M. Kim, and C. M. Lieber, *Science*, **294**, 1313 (2001).

7 a) Z. Yao, H. W. C. Postma, L. Balents, and C. Dekker, *Nature*, **402**, 273 (1999). b) A. Bachtold, A. Hadley, A. Nakanishi, and C. Dekker, *Science*, **294**, 1317 (2001). c) M. S. Fuhrer, J. Nygård, L. Shih, M. Forero, Y. G. Yoon, M. S. C. Mazzoni, H. J. Choi, J. Ihm, S. G. Louie, A. Zettl, and P. L. McEuen, *Science*, **288**, 494 (2000).

8 T. Rueckes, K. Kim, E. Joselevich, G. Y. Tseng, C. L. Cheung, and C. M. Lieber, *Science*, **289**, 94 (2000).

9 a) T. Bjørnholm, T. Hassenkam, D. R. Greve, R. D. McCullough, M. Jayaraman, S. M. Savoy, C. E. Jones, and J. T. McDevitt, *Adv. Mater.*, **11**, 1218 (1999). b) C. Jérôme and R. Jérôme, *Adv. Mater.*, **37**, 2488 (1998). c) S. Choi and S. Park, *Adv. Mater.*, **12**, 1547 (2000).

10 a) D. O. Cowan, "New Aspects of Organic Chemistry," ed by Z. Yoshida, T. Shiba, and Y. Oshiro, Kodansha, Tokyo (1989). b) G. Saito, "Metal-Insulator Transition Revisited," ed by P. P. Edwards and C. N. R. Rao, Taylor & Francis (1995). c) "Organic Conductors," ed by J.-P. Farges, Marcel Dekker, New York (1994). d) T. Nakamura, "Handbook of Organic Conductive Molecules and Polymers," ed by H. S. Nalwa, John Wiley & Sons, New York (1997), Vol. I.

11 F. Favier, H. Liu, and R. M. Penner, *Adv. Mater.*, **13**, 1567 (2001).

12 T. Akutagawa, T. Ohta, T. Hasegawa, T. Nakamura, C. A. Christensen, and J. Becher, *Proc. Natl. Acad. Sci. U.S.A.*, **99**, 5028 (2002).

13 a) Y. Tatewaki, T. Akutagawa, T. Hasegawa, T. Nakamura, and J. Becher, *Synth. Met.*, **137**, 933 (2003). b) H. Miyata, Y. Tatewaki, T. Akutagawa, T. Hasegawa, T. Nakamura, C. A. Christensen, and J. Becher, *Thin Solid Films*, **1**, 438 (2003).

14 T. Akutagawa, K. Kakiuchi, T. Hasegawa, T. Nakamura, C. A. Christensen, and J. Becher, *Langmuir*, **20**, 4187 (2004).

15 a) E. Weber, J. L. Toner, I. Goldberg, F. Vögtle, D. A. Laidler, J. F. Stoddart, R. A. Bartsch, and C. L. Liotta, "Crown Ethers and Analogs," ed by S. Patai and Z. Rappoport, John Wiley & Sons, New York (1989). b) G. W. Gokel, "Crown Ethers & Cryptands" ed by J. F. Stoddart, RSC, Cambridge (1994).

16 a) R. M. Izatt, J. S. Bradshaw, S. A. Nielsen, J. D. Lamb, J. J. Christensen, and D. Sen, *Chem. Rev.*, **85**, 271 (1985). b) R. M. Izatt, K. Pawlak, J. D. Bradshaw, and R. L. Bruening, *Chem. Rev.*, **91**, 721 (1991).

17 a) R. W. G. Wyckoff, "Crystal Structures, Vol. 4," Wiely, New York (1960). b) J. Lima-de-Faria, "Structural Mineralogy. An Introduction," Kluwer, Dordrecht (1994).

18 a) J. B. Torrance, B. A. Scott, and F. B. Kaufman, *Solid State Commun.*, **17**, 1369 (1975). b) J. B. Torrance, B. A. Scot, B. Welber, F. B. Kaufman, and P. E. Seiden, *Phys. Rev. B*, **19**, 730 (1979). c) C. S. Jacobsen, "Optical Properties in Semiconductor and Semimetals. High Conducting Quasi-One-Dimensional Organic Crystals," ed by E. Conwell, Academic Press, New York (1988), p. 293.

19 a) J. B. Torrance, J. E. Vazquez, J. J. Mayerle, and V. Y. Lee, *Phys. Rev. Lett.*, **26**, 253 (1981). b) G. Saito and J. P. Ferraris, *Bull. Chem. Soc. Jpn.*, **53**, 2142 (1980).

20 a) T. Akutagawa, Y. Abe, Y. Nezu, T. Nakamura, M. Kataoka, A. Yamanaka, K. Inoue, T. Inabe, C. A. Christensen, and J. Becher, *Inorg. Chem.*, **37**, 2330 (1998). b) T. Akutagawa, Y. Abe, T. Hasegawa, T. Nakamura, T. Inabe, C. A. Christensen, and J. Becher, *Chem. Lett.*, **2000**, 132. c) Y. Abe, T. Akutagawa, T. Hasegawa, T. Nakamura, K. Sugiura, Y. Sakata, T. Inabe, C. A. Christensen, and J. Becher, *Synth. Met.*, **102**, 1599 (1999).

21 J. B. Torrance, J. J. Mayerle, and K. Bechgaard, *Phys. Rev. B*, **22**, 4960 (1980).

22 M. C. Petty, "Langmuir–Blodgett Films; An Introduction," Cambridge University Press, Cambridge (1996).

23 J. Umemura, T. Kamata, T. Kawai, and T. Takenaka, *J. Phys. Chem.*, **94**, 62 (1990).

24 K. Fukumura, K. Ikeda, and H. Natsuura, *J. Mol. Struct.*, **224**, 203 (1990).

25 M. Meneghetti and C. Pecile, *J. Phys. Chem.*, **84**, 4149 (1986).